PERGAMON

International Journal of Multiphase Flow 28 (2002) 1823–1835

International Journal of Multiphase Flow

www.elsevier.com/locate/ijmulflow

Notes on the path and wake of a gas bubble rising in pure water

A.W.G. de Vries, A. Biesheuvel *, L. van Wijngaarden

J.M. Burgers Centre for Fluid Mechanics, University of Twente, P.O. Box 217, 7500 AE Enschede, The Netherlands

Received 1 June 2001; received in revised form 1 May 2002

Abstract

This paper is concerned with the structure of the wake behind gas bubbles rising at high Reynolds numbers in highly purified water. It describes a schlieren optics technique to visualise the wake. The technique does not contaminate the water, and so does not affect the zero-stress condition at the bubble surface.

It is first shown that zigzagging bubbles have a double-threaded wake of which the axially vorticity components periodically switch sign; some distance downstream of the bubble the wake is unstable. It is explained that this wake structure signifies that the bubble experiences a lift force; the magnitude of the lift force is estimated by two different indirect methods. The results suggest that the zigzag motion is not maintained by periodic vortex shedding, contrary to what was found in earlier investigations.

In the second part of the paper we study the collision of bubbles with a vertical wall. It is shown that in the collision the bubble loses its wake, which subsequently impinges on the wall and reorganises into a coherent, approximately spherical, vortex blob. The presence of vorticity plays a crucial role in the collision. The experimental findings have been incorporated in a simple model to describe the path of a bubble after the collision, which is shown to yield good agreement with what is observed in the experiments.
© 2002 Elsevier Science Ltd. All rights reserved.

1. Introduction

Above a certain volume ($r_{eq} > 0.81$ mm in clean water) bubbles no longer rise rectilinearly: the path becomes a zigzag or a spiral. A similar behaviour is observed for solid spheres, but at lower Reynolds numbers ($Re \approx 200$) than for bubbles ($Re \approx 600$). The boundary conditions at the surfaces of solid spheres and gas bubbles in clean water are different: no-slip and non-deformable

* Corresponding author.

0301-9322/02/$ - see front matter © 2002 Elsevier Science Ltd. All rights reserved.
PII: S0301-9322(02)00036-8

for the solid sphere, zero-tangential-stress and deformable for the gas bubble. These differences influence the vorticity production at the surface and thereby the structure of their wakes and the forces exerted by the surrounding fluid. A slight contamination of the water may seriously affect the free-surface behaviour of a bubble and may make it act like a rigid object.

The literature on the subject of zigzagging and spiralling gas bubbles is extensive (e.g. Saffman, 1956; Lunde and Perkins, 1995; Aybers and Tapucu, 1969; Mercier et al., 1973; Ellingsen, 1998), and the experimental data are inconsistent on various aspects of the bubble motion. One of the reasons may be the continuous bubble release used in some of the experiments, because of which the path of a bubble is influenced by the preceding bubbles, another is the far from smooth release of the bubbles from the top of a needle, causing large deformations and unsteady behaviour of the bubble surface just after the release. We believe that the presence of contaminants in the water in nearly all experiments also plays an important role.

Numerical simulations (Ryskin and Leal, 1984; Blanco and Magnaudet, 1995; Takagi et al., 1997) have confirmed that the vorticity in the flow around a rectilinearly rising gas bubble at large Reynolds number is confined to a thin boundary layer and a thin wake. The regions of the flow carrying vorticity are believed to be much more complex for zigzagging and spiralling bubbles, and the presence of vorticity in the flow presumably plays a much more decisive role in the dynamics. Dye visualisations by Lunde and Perkins (1997), LDA measurements by Ellingsen and Risso (1998) and PIV measurements by Brücker (1999) have shown the existence of vorticity structures behind spiralling and zigzagging bubbles that resemble those found behind solid spheres. The motion of the bubbles was shown to have much in common with that of solid spheres, and it is often also believed that the reasons for the formation of the vortex structures behind the solid spheres and the gas bubbles are the same. Unfortunately the experimental methods used by the authors mentioned above, which require adding dye or seeding with minute particles, are likely to contaminate the water. Since this affects the free surface of the bubble the similarity with the behaviour of solid spheres may be a consequence of the contamination. Whether the results are also relevant for bubbles rising in pure water is an open question.

The present work describes a technique to visualise the wake without affecting the purity of the water (Section 2). We have used this technique to study the vorticity structures behind zigzagging bubbles (Section 3) and bubbles colliding with a vertical wall (Section 4), and based on these observations we devised explanations for the experimentally determined paths of the bubbles.

2. Experimental setup

The experiments were performed in a glass-walled water tank ($15 \times 15 \times 50$ cm, wall thickness 18 mm). Prior to the experiments the tank was intensively cleaned with soap, laboratory ethanol and rinsed with highly purified water. The latter was produced in a three-step purification system consisting of a decalcifier, Millipore RO 60 and a Millipore Q plus. This resulted in water with the highest possible electrical resistance (18.2 $M\Omega\,cm$) and less than 10 ppb organic particles. Contamination of the water was avoided by the use of a closed system and by filling the tank from below. In this way contact with the air and so the absorption of gases, in particular CO_2, is minimised. The bubbles were produced with a system similar to that described in Kok (1993b) and Duineveld (1994). A volume of air is pushed into a transparent silica tube (0.25 mm bore) filled

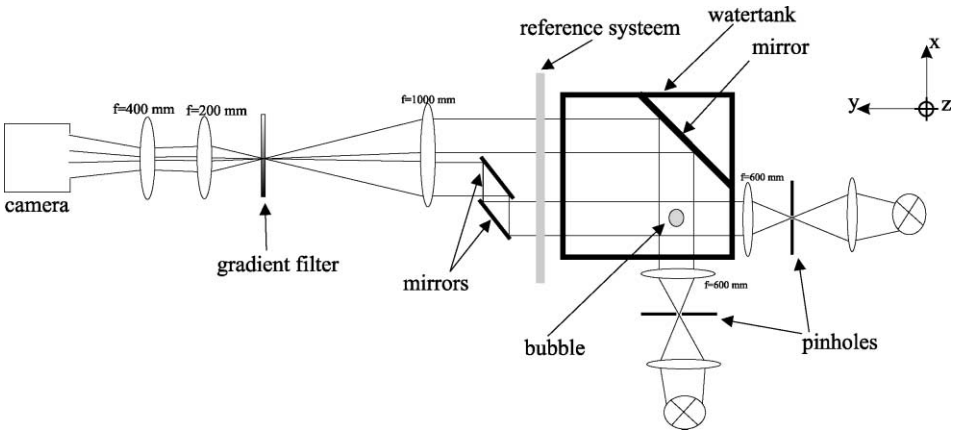

Fig. 1. A sketch of the schlieren visualisation setup. Two perpendicular images are recorded on a single NAC high speed video. A reference system is placed outside the water tank to avoid contact with the water and interaction with the bubbles.

with pure water, is then set on the top of a capillary and subsequently released in a smooth manner. In our application the water in the tank is heated from above by infrared light, which resulted in a constant, stable water temperature gradient (1.1 °C/cm) in the region between 30 and 40 cm above the needle. The colder water, dragged into the wake of the bubble as it rises, is visualised with schlieren optics (Fig. 1). In this way no contamination in the form of particles and/or dye is introduced. The temperature gradient induces an additional buoyancy force on the bubble and a variation of the surface tension along the bubble surface, both effects however can be shown to be negligibly small (de Vries, 2001). The visualisation method is also able to capture simultaneously the outline of the bubble since the refractive index of air differs from that of water. A reference system placed outside the tank is used to correlate the pixel-coordinates with the world-coordinates. Analysing two perpendicular views at the same time, using the Fourier transform method proposed by Lunde and Perkins (1995), yields the position (in 3D), velocity and shape of the bubble.

3. Free rising bubbles

We now discuss our observations of the wake structure behind a zigzagging bubble. Fig. 2 presents a sequence of images obtained for a case in which the plane of the zigzag coincided with one of the projection planes. In the right view the bubble seems to rise along a straight path, that it actually performs a zigzag motion becomes clear from the left view.

The wake has an interesting structure. In the right view (i.e. the *YZ*-view) immediately behind the bubble a double-threaded wake is visible; the left view (the *XZ*-view) only shows a single thread because one thread blocks the view of the other. A little farther behind the bubble the two threads change into a single thread, which subsequently splits and the double-threaded wake reappears. Closer inspection shows that the double-threads are present whenever the curvature of the bubble path is non-zero. When the bubble passes the mean position of the zigzag ($t = 28$ ms in

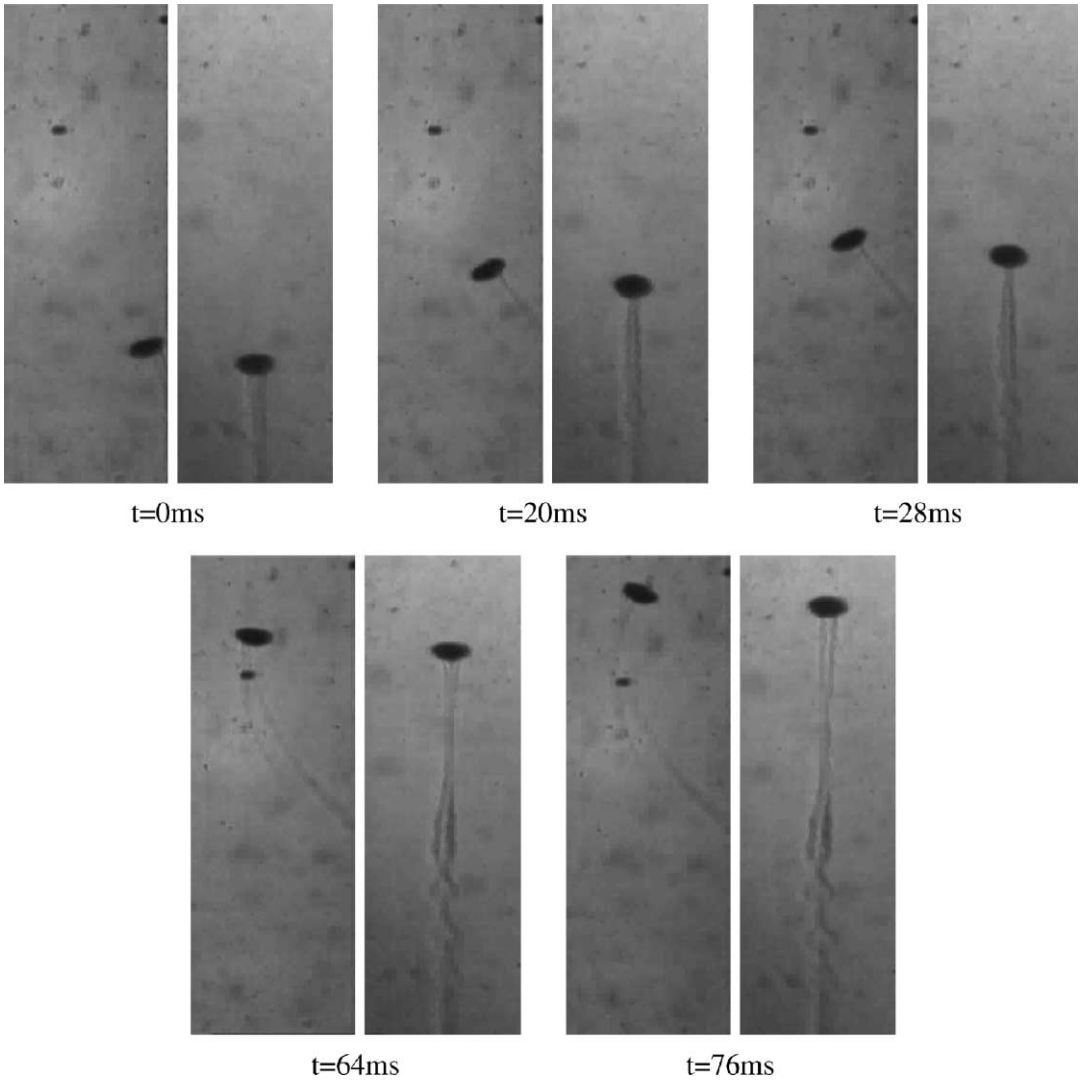

Fig. 2. Successive schlieren images of a bubble ($r_{eq} = 1.00$ mm) in zigzagging motion. In each image the picture on the left shows the *XZ*-plane, that on the right the *YZ*-plane. Immediately behind the bubble the wake has a double-threaded structure where the curvature of the path is non-zero. The threads connect to form a single when the bubble passes through the central position of the zigzag ($t \approx 20$ ms), i.e. where the curvature of the path is zero. Farther downstream the double-threaded wake becomes unstable.

Fig. 2), i.e. when the curvature of the path is zero, a single-threaded wake is produced. Several bubble diameters behind the bubble the double-threaded wake can be seen to undergo an instability and a complex, periodic vortex structure develops. This suggests the following picture: the single-threaded part of the wake carries only azimuthal vorticity, while the vorticity in each of the threads of the double-threaded part of the wake both has an azimuthal component and an axial component, of different sign in each of the threads. If we were to ignore the azimuthal vorticity, the wake immediately behind the bubble would consist of a succession of vortex loops,

which resemble hairpin-type vortices. The loops are formed and closed each time the bubble passes through the symmetry-axis of the zigzag. Apparently the loops develop an instability farther downstream. That the zigzagging motion of the bubbles is maintained by periodic shedding of hairpin-type vortices has also been concluded by other researchers e.g. Lunde and Perkins (1997) and Brücker (1999); note however that these authors suggest that the vortex loops are formed and closed when the bubble is farthest removed from the centre-line of the zigzag.

Given the fact that at a certain moment a double-threaded wake is found behind the bubble it is clear why the path is then curved. Associated with this wake structure is a fluid velocity normal to the direction of motion. As the bubble moves forward new elements of the wake are added, and the corresponding change of the momentum carried by the wake implies that a lift force is exerted on the bubble in the opposite direction. This force, normal to the direction of motion, will cause the bubble to follow a curved path. Why the double-threaded wake is present is less clear. A rectilinearly rising bubble has a symmetrical shape and it moves along the symmetry-axis. The vorticity in the fluid is confined to a thin boundary layer and the wake. The threads of the double-threaded wake carry vorticity with an axial component, which suggests that at the bubble surface a meridional vorticity component is generated. This can be a consequence of the deformation process of the bubble as it adjusts its shape such that the symmetry-axis remains along the direction of motion when it follows the curved path, effectively a solid body rotation around an axis normal to the symmetry-axis; a small departure of the symmetrical shape or a slight tilt of the symmetry-axis away from the direction of motion may also be involved. The resolution of our experimental technique is as yet insufficient to settle these matters; it might be noted that Ellingsen (1998) claims that the symmetry-axis is aligned with the bubble path.

Our visualisation method gives a picture of the structure of the wake; it does not reveal the accompanying velocity field. This means that the strength of the vortex filaments forming the wake cannot be determined directly. We have tried to estimate this by several indirect methods. The first method uses the self-induced motion of a double-threaded wake. Instead of a zigzagging motion bubbles of the same range of sizes can also perform a spiralling motion. Experiments show that in that case the wake also has a double-threaded structure, which however is less prone to become unstable. To obtain an estimate of the velocity of the self-induced motion the wake behind a spiralling bubble is better suited. If the self-induced velocity of the vortex filaments is U_f and the distance between them is l the circulation Γ of the vortex filaments can be estimated from $\Gamma = 2\pi U_f l$. The associated lift force can then be estimated by

$$L = \rho \Gamma l U_T = 2\pi \rho U_f l^2 U_T, \tag{1}$$

where U_T is the mean rise velocity of the bubble. For a typical experiment with a bubble of radius $r_{eq} = 1.0$ mm the following values were found, by inspection of the schlieren images:

$$U_f \approx 3.5 \text{ cm/s}, \quad U_T \approx 31.6 \text{ cm/s}, \quad l \approx 0.6 r_{eq} = 0.6 \text{ mm}.$$

This results in a lift force $L \approx 2.5 \cdot 10^{-5}$ N. (Note that in obtaining this result we have accounted for the 29° pitch angle of the spiral.)

A second method of estimating the lift force is by looking at the angle between the path and the vertical at the mean position of the zigzag, i.e. when the curvature of the path is zero and the wake consists of a single thread. Precisely at that moment the lift force vanishes, but immediately before that there exists a balance between the component of the buoyancy force normal to the path and

the lift force. The experiments show that for a bubble with an equivalent radius $r_{eq} = 1.0$ mm this angle is approximately 36°. With a liquid density $\rho = 1000$ kg/m^3 and the gravitational acceleration $g = 9.81$ m/s^2 we find that the buoyance force component is $\rho g 4/3\pi r_{eq}^3 \sin(36) = 2.4 \times 10^{-5}$ N; in good agreement with the estimate of the lift force determined from the self-induced motion of the wake.

4. Bubbles bouncing against a vertical wall

The second part of our study is concerned with the collision of bubbles against a vertical wall. The experimental setup is that described in Section 2, but now with a glass wall placed in the middle of the tank; the lower edge 10 cm above the bottom of the tank and 4 cm above the tip of the capillary, to ensure that the bubble reaches its terminal rise velocity before interacting with the wall (Fig. 3). The direction normal to the wall will be denoted x and that along the wall y; the corresponding velocity components are u and v, respectively. The horizontal distance between the wall and the capillary is s_i.

Fig. 4 shows examples of the observed bubble trajectories for a fixed $s_i = 1.57$ mm. Typically four types of motion are observed, when the bubble size is increased: (i) after the collision the bubble slides along the wall, (ii) the bubble bounces repeatedly, (iii) after the bounce the bubble moves slowly away from the wall, (iv) the bubble bounces repeatedly with an amplitude that is considerably larger than the initial distance from the wall. In the case shown here the small bubbles ($r_{eq} = 0.41$ and 0.43 mm) actually do not collide with the wall and then slide along it. The

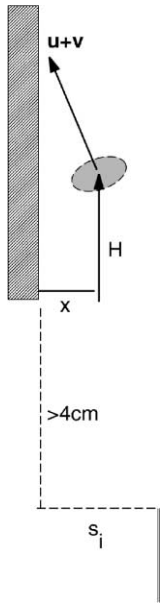

Fig. 3. Sketch of the setup used to study bubble collsions with a vertical wall. The lower edge of the vertical wall is at least 4 cm above the tip of the capillary. The horizontal distance of the capillary to the wall, s_i, is adjustable. The coordinate normal to the wall is denoted x, that along the wall y.

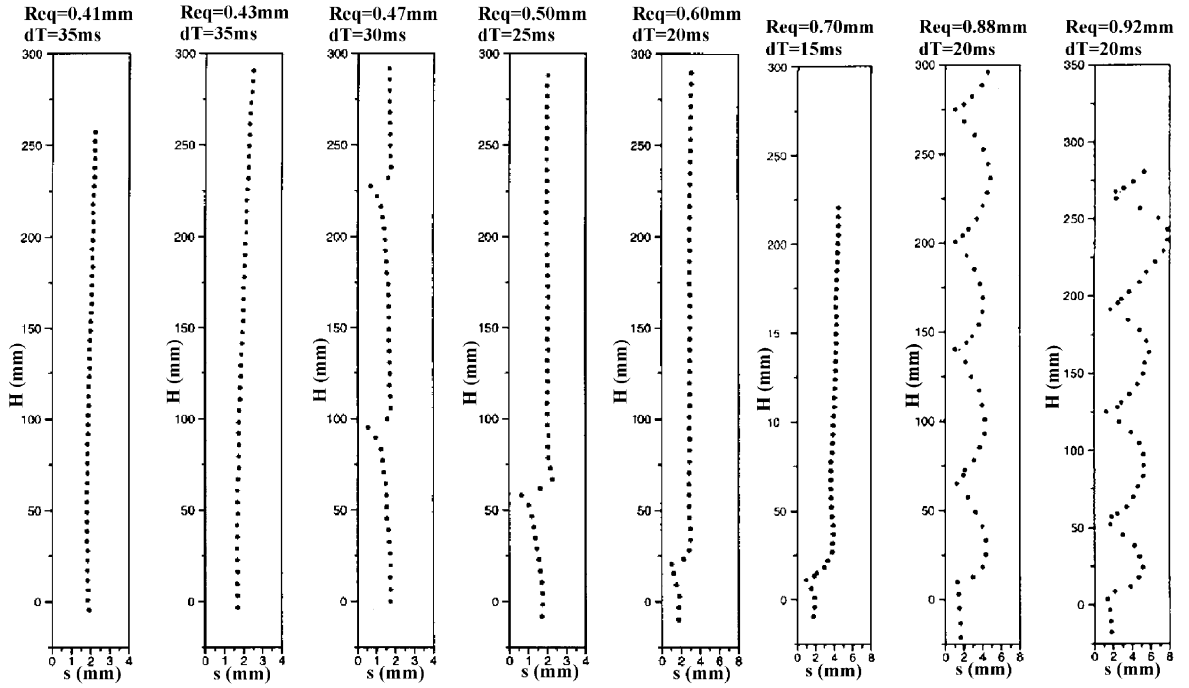

Fig. 4. Experimentally determined trajectories of bubbles of different sizes as they interact with a vertical wall. In all cases the initial separation $s_i = 1.57$ mm.

simple model presented below suggests that a possible explanation for this is a small tilt of the wall. Even a tilt within the experimental accuracy of 0.2° appears to be sufficient to induce a gravitational force component normal to the wall that outweighs the attractive force towards the wall due to the image system of the bubble within the wall.

Bubbles of about $r_{eq} = 0.47$ mm are observed to bounce repeatedly with an amplitude that is approximately equal to s_i. Which type of motion occurs after the first collision, (i) sliding or (ii) repeated bouncing, appears to be determined by a Weber number based on the approach velocity between the bubble and its image. The critical value is $We_{cr} = 0.165$. This compares well with the $We_{cr} = 0.18$ found by Duineveld (1994) which determines whether two rising gas bubbles coalesce or bounce after a collision.

The third type of motion, a slow separation after the collision with the wall, is observed for $r_{eq} = 0.50$, 0.60 and 0.70 mm. Again, this is a consequence of the slight tilt of the wall. After the bounce the bubble reaches a distance from the wall that is so large that the the attractive force towards the wall becomes less than the small gravitational force away from the wall.

When the bubble size is increased further, for a fixed $s_i = 1.57$ mm, a new phenomenon is observed. The largest bubbles, $r_{eq} = 0.88$ and 0.92 mm, are now not completely repelled from the slightly tilted wall by the gravitational force, but again bounce repeatedly, now with very large amplitudes. These amplitudes and the distances travelled between the bounces are not constants; see for example the fourth bounce for $r_{eq} = 0.92$ mm. The critical parameter that characterizes the transition from the third type of collision to the fourth turns out to be the same critical parameter

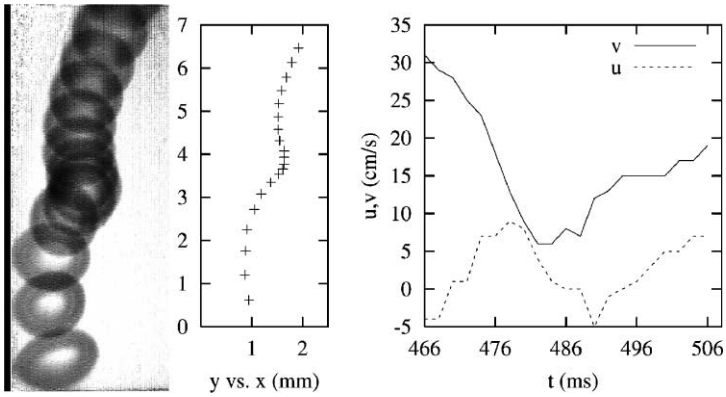

Fig. 5. The first collision of a bubble with radius $r_{eq} = 0.84$ mm with a vertical wall; $s_i = 1.5$ mm. The picture on the left is obtained by superposition of separate frames with a 4 ms time difference. The graphs give the position (middle) and the velocity of the centre of the bubble (right).

that signifies the transition from rectilinear motion to zigzagging or spiralling motion of free rising bubbles. In the fourth type of collision the bubbles have a double-threaded wake, and the bubbles experience a lift force with a component that is always directed towards the wall and that resists the repelling gravitational force.

We now describe in more detail the path of the bubble when it is very close to the wall. In Fig. 5 the bubble behaviour is displayed by presenting the images obtained with a 4 ms time difference in one figure. The corresponding bubble positions and velocities are also shown. The first bubble (lowest, $t = 466$ ms) is about to hit the wall. It has an oblate ellipsoidal shape with a minor axis that coincides with the direction of motion of the bubble. The ratio between the velocity along the wall and that normal to it is large: numerically differentiation of the path gives a vertical velocity of 32 cm/s and a horizontal velocity of −6 cm/s just before bouncing. Only 4 ms later, immediately after the collision, the bubble shape has changed significantly and has become nearly spherical. First the bubble appears to slide for a very short moment along the wall, while its vertical velocity slowly decreases. Soon after ($t = 8$ ms), the bubble moves a little away from the wall, and now the vertical velocity drops considerably, from 23 cm/s to about 6 cm/s. At $t \approx 16$ ms the bubble motion is purely vertical. Next, the bubble distance to the wall decreases slightly, the vertical velocity remaining small. Finally, the bubble accelerates upwards and moves away from the wall quickly.

Flow visualisation with the previously described schlieren optics technique, and with a linear water temperature gradient, gives a few indications why this peculiar bubble motion happens. The images presented in Fig. 6 are for an initial distance of $s_i = 1.57$ mm (as those in Fig. 4), but the behaviour in that case is similar to that for $s_i = 1.50$ mm (Fig. 5). They show the formation of a vortical region that consists of the vorticity accumulated at the rear of the bubble, which is shed as the bubble collides with the wall, the vorticity in the wake impinging on the wall and, presumably, some of the vorticity of the boundary layer that is formed at the wall. After the bubble has bounced, the vortical region develops into a roughly spherical blob. This blob then moves upwards with a velocity that increases to a final value that is estimated as $0.2U_T$, where U_T the terminal rise velocity of the bubble. Let us now try to relate these observations with the behaviour

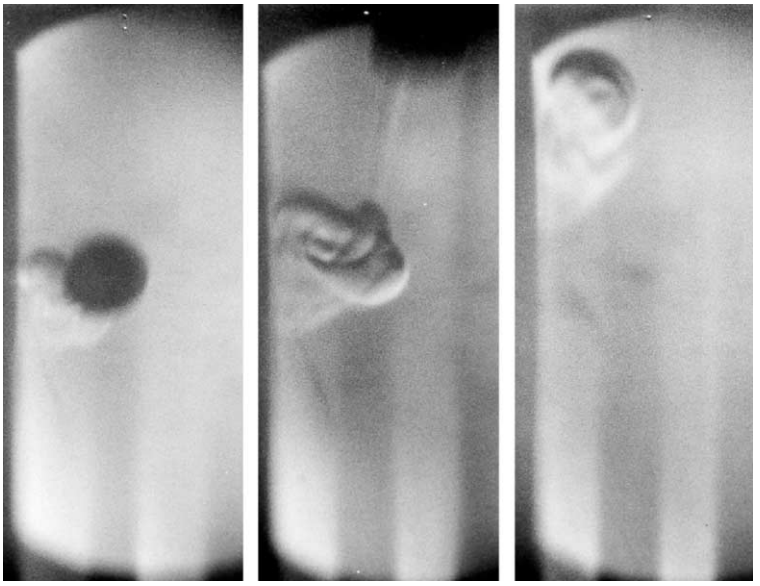

Fig. 6. Schlieren images of the formation of a vortical region when a bubble ($r_{eq} = 0.85$ mm) collides with a vertical wall. The time intervals between the consecutive images are 26 and 60 ms. Note the upward motion of the vortex blob.

shown in (Fig. 5). Note that during the collision the bubble velocity is significantly reduced, not however simply due to viscous shear as the bubble slides along the wall: the major reduction takes place when the bubble is slightly removed from the wall. What happens presumably is that at first ($t = 0$–12 ms) the wake that has been shed during the collision and that subsequently impinges on the wall, moves in between the bubble and the wall, thereby pushing the bubble forwards as it slides along the wall and displacing it slightly away from the wall. By the time the roughly spherical vortex blob has been formed the bubble is in a position above and slightly to the right of the vortex blob. In that position the slowly moving blob induces a velocity field at the position of the bubble which exerts a force on the bubble that attracts it towards the blob. As a consequence the bubble moves a little bit to the wall ($t = 20$ ms) and also its upward velocity is strongly reduced.

It is worth trying to include these findings in an analytical model from which the bubble motion can be calculated. As a simple starting point we assume the bubbles to have a spherical shape, and we adopt the method used e.g. by Kok (1993a). In this viscous potential flow model the inertia forces are derived using the Lagrange formalism, which includes a Rayleigh dissipation function to find an expression for the viscous drag; the effects of hydrodynamic interactions are also taken into account. For the case of a bubble bouncing with a vertical wall, and when only dipole contributions are taken into account, Kok's equations of motion reduce to

$$\begin{aligned} \rho V \frac{\mathrm{d}M_y \dot{y}}{\mathrm{d}t} &= F_y, \\ \rho V \frac{\mathrm{d}M_x \dot{x}}{\mathrm{d}t} &= \frac{1}{2}\rho V \left[\dot{y}^2 \frac{\mathrm{d}M_y}{\mathrm{d}x} + \dot{x}^2 \frac{\mathrm{d}M_x}{\mathrm{d}x} \right] + F_x, \end{aligned} \tag{2}$$

where x is the distance from the wall, y is the distance along the wall, V is the volume of the sphere, M_x and M_y are the added mass coefficients and F_x and F_y the external forces acting on the pair of spheres. In Kok's model the external forces are due to buoyancy and viscous drag:

$$M_x = 1 + \frac{3}{8}\left(\frac{r_{eq}}{x}\right)^3, \quad M_y = 1 + \frac{3}{16}\left(\frac{r_{eq}}{x}\right)^3, \tag{3}$$

$$F_x = 24\pi\nu r_{eq}\dot{x}\left(1 + \frac{1}{4}\left(\frac{r_{eq}}{x}\right)^3\right), \tag{4}$$

$$F_y = 2\rho g V + 24\pi\nu r_{eq}\dot{y}\left(1 + \frac{1}{8}\left(\frac{r_{eq}}{x}\right)^3\right). \tag{5}$$

These equations give an accurate description of the bubble motion up to the first collision against the wall, but fails to describe the various types of motion after this collision. The model can be improved by incorporating (i) a criterion that determines whether the bubble slides along the wall or bounces after a collision, (ii) the large reduction in the upward velocity during a collision, (iii) a gravitational component normal to the wall when the wall is slightly tilted, and (iv) a criterion that determines whether the bubble will experience a lift force as it rises. The criterion for the transition between sliding and bouncing was shown above to be the critical Weber number $We_{cr} = 0.165$. When $We > 0.165$ the bounce is modelled as an elastic collision in the direction normal to the wall, and a no-slip condition is supposed to hold in the direction along the wall: $(u \to -u, v \to 0)$. The case of sliding, $We < 0.165$, the bounce is modelled as an elastic collision in both direction $(u \to -u, v \to v)$. The bounce amplitude is then quickly damped by dissipation, so that $u \to 0$. For simplicity we took $r_{eq} > 0.80$ as the criterion for the presence of a lift force on the bubbles, a criterion that applies for bubbles rising in water at 20 °C, and estimated, as suggested by the experiments described in Section 3, the lift force as given by $L = \pi\rho r_{eq}^2 U_T^2/13$. Examples of bubble trajectories calculated with this model are shown in Fig. 7, for an initial separation distance $s_i = 1.57$ mm as was used in the experiments, and with a tilt angle of the wall of 0.1°. The qualitative agreement with the experiments is promising, note in particular the nose-shaped trajectories when the bubble bounces repeatedly. Also the amplitudes of the bounces agree reasonably well with the observations. By including the effects of bubble shape deformations on the inertial coefficients and the drag forces, an even closer agreement can perhaps be obtained, but this is far from simple.

We conclude this section by noting that the strong reduction in the vertical bubble velocity effectively results in a large (up to 97%) loss of kinetic energy at bouncing. For the bouncing bubble presented in Fig. 5 the kinetic energy just after the collision is reduced to $u^2/(u^2 + v^2) \approx 4\%$ of the value just before the collision. Since the attractive force due the mirror bubble in the wall is proportional to the bubble velocity magnitude squared, immediately after the collision that attractive force is much smaller than it was just before the collision. However, the magnitude of the velocity normal to the wall is unchanged and so with a smaller force to slow down the bubble as it moves away from the wall, the bubble may reach separations from the wall that are larger than those it had initially. Remarkably, a loss of energy in the collision may lead to an increase in the amplitude of the bounce.

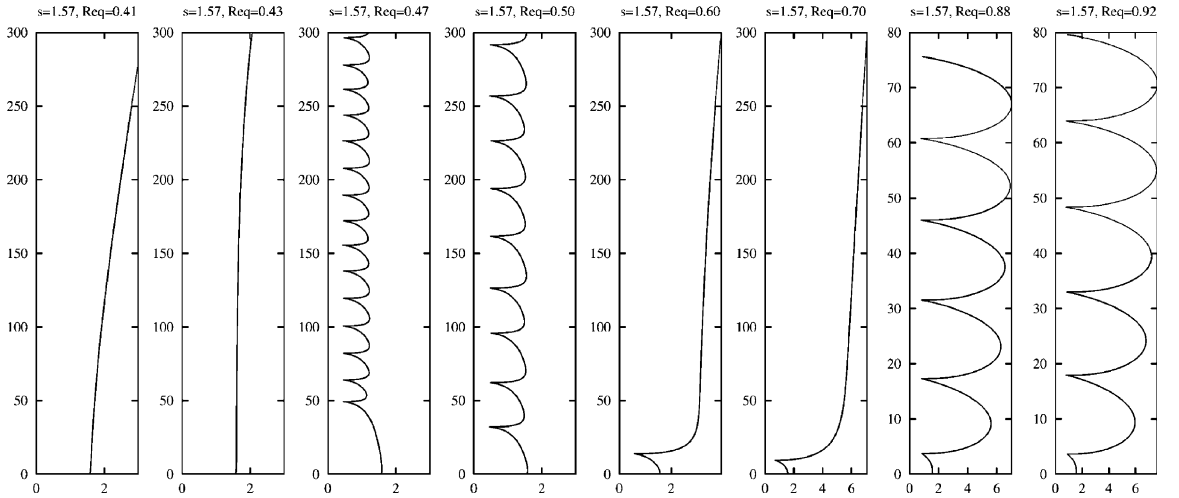

Fig. 7. Results of the approximate model for the collisions of bubbles with a vertical wall. The initial separation $s_i = 1.57$ mm, the wall is tilted with an angle of 0.1° with respect to the vertical. As in Fig. 4 the origin is at the bottom edge of the plate and distances are measured in mm.

5. Conclusions

The main purpose of this study is to understand more about the dynamics of rising bubbles. We believe that the path of a bubble, when it performs a zigzagging or spiralling motion, is correlated with the structure of the wake behind the bubble, which in turn is affected by the purity of the water. Discrepancies between various experimental observations published in the literature are presumably caused by differences in the amounts of impurities in the water, and so we devised a method of visualising the wake without affecting the water purity. The idea is to introduce a stable, small temperature gradient in the water, and to visualise the wake by a schlieren optics technique.

It was observed that free rising bubbles in zigzagging motion (and also in spiralling motion) carry a double-threaded wake, consisting of two counter-rotating vortex filaments. This wake occurs whenever the curvature of the path is non-zero, and associated with it is a lift force directed to the centre of curvature of the path. By two different indirect methods we estimated the magnitude of the lift force, and the results are in good agreement. At the central position of the zigzag, where the curvature of the path is zero, the double-threaded wake disappears, and the wake for a brief moment consists of a single thread. When the curvature of the path becomes non-zero again, the double-threaded reappears, now with the signs of the trailing vorticity, and so also the lift force, switched. This suggests that the zigzagging motion is maintained by periodic shedding of vortex loops, that resemble hairpin-type vortices. At a considerable distance behind the bubble the double-threaded wake becomes unstable; the instability leads to the formations of vortex blobs.

The vorticity in the flow around a rising gas bubble also has a strong effect on the collisions of gas bubbles with a vertical wall. Typically four types of collision have been found: (i) the bubble slides upwards along the wall after the collision, (ii) the bubble bounces repeatedly with an amplitude of the order of the initial separation distance to the wall, (iii) the bubbles bounces from the

wall and then moves away from it, (iv) the bubble bounces repeatedly with an amplitude much larger than the initial separation distance.

The parameter determining the transition between the first two types of collision is a Weber number based on the approach velocity. Its critical value is ($We_{cr} = 0.165$), which is close to the value ($We_{cr} = 0.18$) found by Duineveld (1994) that determines whether two rising bubbles coalesce or bounce after a collision. Our experiments show that when bubbles bounce against the wall, the velocity component along the wall is significantly reduced, predominantly as a consequence of the velocity field induced by a vortex blob that is formed at the wall; a blob that consists of the vorticity that was originally in the wake close to the bubble. The result is that the force that attracts the bubbles towards the wall is also reduced significantly, so that after the bounce the bubbles may reach distances from the wall that are larger than the initial separation distance. A small tilt of the wall effectively gives rise to a component of the buoyancy force away from the wall. This may outweigh the attractive force towards the wall; this is the reason for the third type of motion we observed. The parameter that signifies the transition from the third to the fourth type of collision is the same as that which determines whether the rectilinear motion of a free rising bubble is unstable. In the fourth type of collision process the lift force associated with the doubled-threaded wake plays an important role. When bouncing, the centre of curvature of the path is on the side that faces the wall, which means that the lift force attracts the bubbles towards the wall; together with the small tilt of the wall, and the above described reduction of the vertical velocity at collision, this explains that in the fourth type of collision the repeated bouncing occurs again, now with a large amplitude.

These deductions from the experimental observations have been incorporated in a simple model to calculate the bubble trajectories before and after a collision with a wall. The model is an extension of that formulated by Kok (1993a). Although it assumes that the bubbles have a spherical shape, it gives results that are in qualitative agreement with the experiments, in particular the peculiar 'nose-like' shape of the bubble path is reproduced and the amplitudes of the repeated bounces are of the correct order of magnitude.

A much more elaborate report on this work may be found in the thesis of one of the authors (de Vries, 2001) or in a paper that is under preparation.

References

Aybers, N.M., Tapucu, A., 1969. The motion of gas bubbles rising through stagnant liquid. Wärme und Stoffübertragung 2, 118–128.

Blanco, A., Magnaudet, J., 1995. The structure of the axisymmetric high-Reynolds number flow around an ellipsoidal bubble of fixed shape. Phys. Fluids 7, 1265–1274.

Brücker, C., 1999. Structure and dynamics of the wake of bubbles and its relevance for bubble interaction. Phys. Fluids 11, 1781–1796.

Duineveld, P.C., 1994. Bouncing and coalescence of two bubbles in water. Ph.D. Thesis, University of Twente.

Ellingsen, K., 1998. Hydrodynamique des écoulements pilotés par l'ascension de bulles d'air virevolantes. Ph.D. Thesis, Institute National Polytechnique de Toulouse.

Ellingsen, K., Risso, F., 1998. Measurements of the flow field induced by the motion of a single bubble. In: Proc. Third Int. Symp. on Multiphase Flows, Lyon.

Kok, J.B.W., 1993a. Dynamics of a pair of gas bubbles moving through liquid. Part I. Theor. Eur. J. Mech. B/Fluids 12, 515–540.

Kok, J.B.W., 1993b. Dynamics of a pair of gas bubbles moving through liquid. Part II. Experiment. Eur. J. Mech. B/Fluids 12, 541–560.

Lunde, K., Perkins, R.J., 1995. A method for the detailed study of bubble motion and deformation. In: Serizawa, A., Fukano, T., Bataille, J. (Eds.), Advances in Multiphase Flow. Elsevier Science Publishers, pp. 395–405.

Lunde, K., Perkins, R.J., 1997. Observations on wakes behind spheroidal bubbles and particles. No. FEDSM97-3530. ASME-FED Summer Meeting, Vancouver.

Mercier, J., Lyrio, A., Forslund, R., 1973. Three-dimensional study of the nonrectilinear trajectory of air bubbles rising in water. Trans. ASME J. Appl. Mech. 40, 650–654.

Ryskin, G., Leal, L.G., 1984. Numerical solution of free-boundary problems in fluid mechanics. Part 2. Buoyancy-driven motion of a gas bubble through a quiescent liquid. J. Fluid Mech. 148, 19–35.

Saffman, P.G., 1956. On the rise of small air bubbles in water. J. Fluid Mech. 1, 249–275.

Takagi, S., Matsumoto, Y., Huang, H., 1997. Numerical analysis of a single rising bubble using boundary-fitted coordinate system. JSME B 40, 42–50.

de Vries, A.W.G., 2001. Path and wake of a rising bubble. Ph.D. Thesis, University of Twente.